INVESTIGATION OF A BULK METALLIC GLASS AS A SHAPED CHARGE LINER MATERIAL

Laszlo J. Kecskes[1] and William P. Walters[2]

U.S. Army Research Laboratory
Weapons and Materials Research Directorate
[1]AMSRD-ARL-WM-MB
[2]AMSRD-ARL-WM-TC
Aberdeen Proving Ground, MD 21005, USA

Vitreloy 106 is a zirconium (Zr)-based bulk metallic glass (BMG) with a nominal composition of $Zr_{57}Nb_5Cu_{15.4}Ni_{12.6}Al_{10}$ (at.%), or $Zr_{67.95}Nb_{6.07}Cu_{12.79}Ni_{9.66}Al_{3.53}$ (wt.%). It has a density of 6.7 g/cm^3. At present, BMG have found multiple applications, but these materials were never investigated regarding their potential use as shaped charge liner materials. Consequently, an experimental program was designed to evaluate the jetting behavior of Vitreloy 106 under a variety of conditions. The study showed that the Zr-based BMG behaved more like a shaped charge liner fabricated from pressed powdered metals than those made from pure glass.

INTRODUCTION

The use of a material as a shaped charge liner means that it will be subjected to extremely high strains, strain rates, pressures, and temperatures [1]. In general, the behavior of any material during these conditions is not known. Historically, the best shaped charge liner materials are pure metals [1]. On one hand, alloys of metals, with a few exceptions, do not form ductile coherent jets, and the jet is diffuse or spreads over time. On the other hand, jets that are fluid in nature do not particulate or break into particles as most metallic jets do. Simple oxide glass liners also perform well, but their penetration is low because of the low density of the jet. Shaped charge liners fabricated from pressed powders (usually a tungsten, copper, graphite mixture), such as those used in the oil well industry, are coherent but tend to dissipate over time [2]. For the oil well industry, this is not a major problem since the jet engages the target at short stand-off distance. Vitreloy 106, a common bulk metallic glass (BMG) with a nominal composition of $Zr_{57}Nb_5Cu_{15.4}Ni_{12.6}Al_{10}$ (at.%), or $Zr_{67.95}Nb_{6.07}Cu_{12.79}Ni_{9.66}Al_{3.53}$ (wt.%), was assumed to behave somewhat like a powder liner because of its composition. Vitreloy 106 has a density of 6.7 g/cm^3. With ultrasound measurements, it was

determined that this BMG has a longitudinal wave velocity of 5350 m/s, a shear wave velocity of 2420 m/s, and thus a bulk sound velocity of 4562 m/s [3]. For comparison, copper has a density of 8.9 g/cm^3 and a bulk sound velocity of 3980 m/s. The current study was an attempt to determine the exact nature of the jetting behavior from a shaped charge liner of Vitreloy 106.

EXPERIMENTAL PROGRAM

Shaped Charge Liner Geometry

Three conical shaped charge liners were fabricated by injection molding at Howmet Corporation [4] for the U.S. ARDEC. The liners had typically 86.9-mm outer diameter, 106.1-mm altitude, with a nominal 42-degree apex angle. The conical liners had a cylindrical knob or plug at the apex which was 8.3 mm high and 12.8 mm in diameter. The liners proved to be “non-precision” in that the outer base diameter varied as much as 0.25 mm and the apex angle varied by as much as 0.5 degree among the three liners. Previously, X-ray radiography has indicated pores or voids near the apex but no macro flaws in a fourth liner. This was not verified for each of the three liners.

Firing Program

The liners were loaded with finely grained OCTOL (65% Cyclonite [RDX] and 35% trinitrotoluene [TNT]) and vacuum cast. The charge diameter (CD) was 101.6 mm and the cylindrical OCTOL billet was 190.5 mm high. The uncased liner weight varied from 2675 to 2780 g. The variation in weights was attributable to the lack of precision in the liners.

The first two shots were designed to determine the free-flight jet characteristics, and the final shot was for penetration. The experiments were conducted at the using two 150-keV X-rays for the early flash times with orthogonal flashes and three 450-keV X-rays for the later times.

Shot #3618 was the first round tested against a stack of 25.4-mm-thick rolled homogeneous armor (RHA) witness plates (target). The stand-off distance was 2845 mm or 28 CDs. The result was a splatter on the first witness plate. Shot #3619 was the second free-flight radiography test designed to examine the jet more closely now that the tip velocity was accurately known. The stand-off distance was lowered to 1401 mm or 13.8 CDs. The result was perforation of the first witness plate. The final shot #3620 was designed only for penetration at a shorter stand-off distance. The stand-off distance was 203.2 mm or two CDs and the penetration depth was 232.6 mm.

Sample Analysis

A small section from one of the liners was chemically analyzed to verify its composition and detect any impurities that may affect its glass-forming ability. It is well known that excessive amounts of oxygen and carbon interstitials (e.g., above 100 ppmw) in a bulk metallic alloy strongly affect how readily the alloy can be quenched into a vitreous state [5]. Metal components were measured with direct current plasma emission spectroscopy, carbon with combustion infrared detection, whereas oxygen and nitrogen were measured with inert gas fusion.

After the completion of the three firing tests, the plates were photographed and sectioned to examine the interaction surface between the steel and the Vitreloy 106 liner material. Sectioned pieces were further cut, cleaned of rust, and sequentially polished for scanning electron microscopy and trace elemental identification by energy dispersive X-ray analysis.

RESULTS AND DISCUSSION

Jet Radiography and Overall Target Plate Appearance

Shot #3618 The flash radiographs from the shot are shown in Figure 1. In the figure, the jet travels from right to left. The first appearance of the jet at the earliest flash time shows the jet with a large bulb-like tip. In the next flash, the jet bifurcates or comes apart at the tip and begins to dissipate. At the last flash time, the jet nearly disappears. This is typical of powder jets. Figure 1(b) shows an enlarged version of the jet at an earlier time. There were gaps or hollow regions in the jet which may indicate the presence of voids in the liner. Another effect of void or non-uniformity in the cast liner is manifested in the large variation of particulate size in the jet.

The penetration was small. The jet impacted the lower left-hand corner of the witness plate; the maximum hole depth was 19 mm. The jet tip velocity was measured to be 8.3 km/s. This result is consistent with the flash X-ray in that the jet was not straight and was diffuse. Figure 2(a) shows the impact region. The lack of any bulging on the rear of the plate, testifies to the incompleteness of the penetration into the plate. It is difficult to discern the damaged region of the front side of the plate in the macro photograph. Figure 2(b) shows a closer view of the sectioned lower left corner with a clear demonstration of fragments peppering the plate surface without any appreciable penetration. The random pitting is consistent with the incoherent jet impacting the plate surface. Most of the pits were shallow, about 1 to 3 mm in diameter; though, some of the pits were larger (12 to 15 mm). Larger pits sometimes contained small but heavily oxidized liner material. The discoloration was bluish, likely from staining and adhesion of possibly molten liner material.

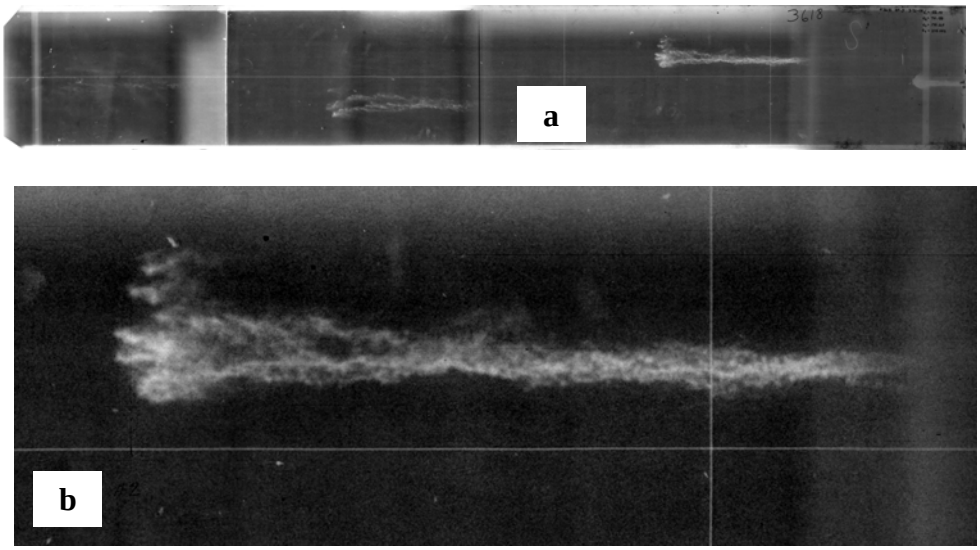

Figure 1. Multiexposure flash X-ray radiograph of Shot #3618 in (a); key section of the jet in (b). Note the extensive particulation, dispersion, and diffusion of the jet.

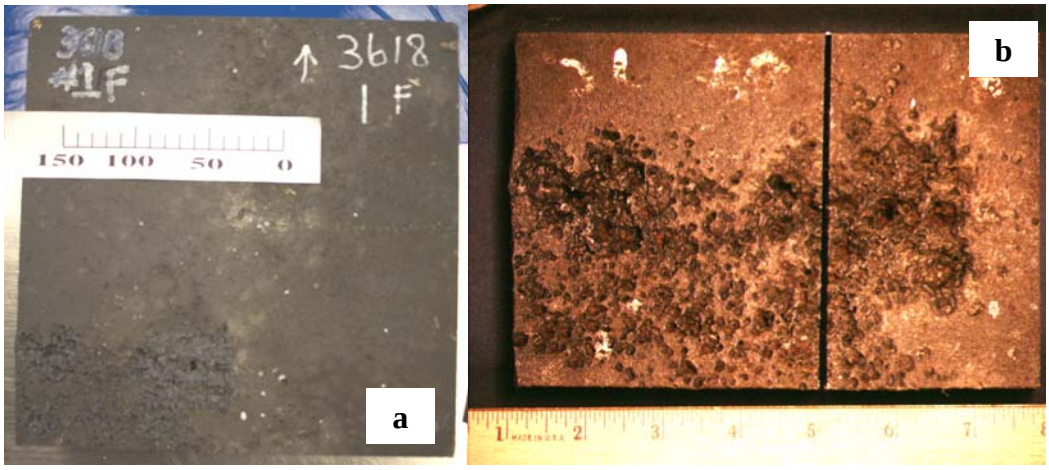

Figure 2. Macrophotograph of the impacted target plate in (a); enlarged view of the pitted surface in (b).

Shot #3619 This jet also exhibited a "powdery" appearance with evidence of voids in the jet. The jet dissipated at later times and was not straight. Because the jet bifurcated, there were multiple impacts present. Using a shorter stand-off distance, the

penetration was greater than 25.4 mm, i.e., the jet penetrated the first witness plate and entered the second plate about 15 mm. The holes were irregular because of the diffuse nature of the jet. The inside surface of the hole wall was rough with liner material adhering to it. Again, fine, blue-colored debris coated the walls. The cavity bottoms in the second plate had small, blue particles.

The depth of penetration from the liner was much improved and damage was more extensive, but the appearance of the affected surfaces was similar to that described previously. Some of the fragments had rounded edges with a molten appearance. These surfaces were clearly a result of a combination of particulate erosion, impact, and dynamic flow.

Shot #3620 In the final shot, the jet penetrated nine 25.4-mm plates and 4 mm into the tenth plate for a total penetration of 232.6 mm or 2.3 CD. This penetration depth is not impressive but indicative of powder jets in that the best penetration is achieved at short standoff. The entrance hole (first target plate) was relatively large (about 52.0 mm), and the holes were nearly circular. Examination of the hole profiles in each of the target plates revealed that unlike those seen in the previous two shots, the last shot produced a considerably smoother surface finish. The erosion surfaces were again discolored, but the coloration was less intense, indicative of perhaps less residual liner material on the walls. The plates were cut and Figure 3 illustrates the penetration profile of the tunnel created by the jet.

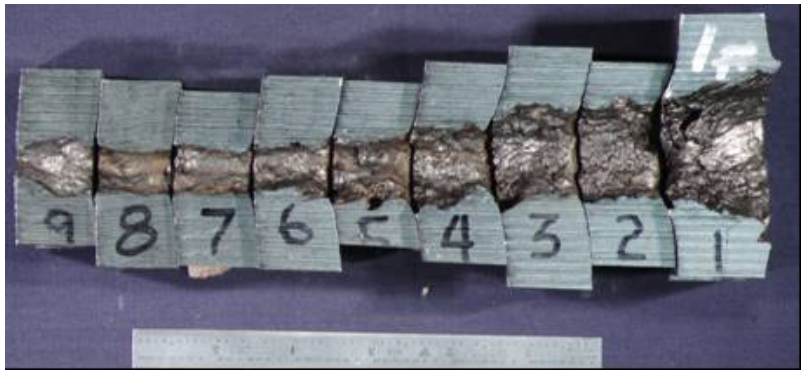

Figure 3. Cross-sectional view of the #3620 target block showing the penetration tunnel.

Results obtained in the first two experimental shots, show early dispersion of the jet during the initial collapse and flight causing the alloy material to be less effective by the time it reached the target stack. Elimination of the large stand-off distance reduced the previously observed excessive dispersion of the liner material and, penetration effectiveness improved. That is, more of the jet's kinetic energy was converted into

penetration depth. The jet in the third test generated much smoother erosion surfaces. Although no large-scale debris or particulate matter was found on these latter surfaces, the tell-tale bluish discoloration was still present. Nevertheless, the smooth surface of the penetration tunnel from shot #3620 also indicated that unlike the long stand-off scenarios of shots #3618 and #3619, the erosion by the dispersed jet was more effective.

Analysis of the Target Plate Surfaces

As the particulated jet erodes the surface and comes to rest in the target cavity, because of subsequent latent heating in the target and availability of heat, the metallic glass may undergo partial or complete melting. Typically, when a vitrified metallic glass is heated above its glass transition temperature, its viscosity decreases several orders of magnitude. Then, it is not unreasonable to expect that this viscous solid could easily flow over the free surface of the steel target given enough time. As presented in Figures 4 and 5, the metallic glass liner at some time flowed, coated, and alloyed with the steel witness plate. The intermixed region contained voids, cracks, and extensive crystalline structures. Qualitative X-ray analysis revealed both elemental components of the metallic glass and steel. Within the alloy material, there was less Fe present, whereas, in the subsurface steel region, analysis showed Fe and Mn, consistent with the composition of RHA. Cracks along the interface between the steel and metallic glass layer likely formed because of strong differences between thermal properties of the materials during cooling.

Vitreloy 106 has a nominal composition of $Zr_{57}Nb_5Cu_{15.4}Ni_{12.6}Al_{10}$ (at.%), but chemical analysis revealed that the actual composition, $Zr_{50.4}Nb_{3.1}Cu_{15.7}Ni_{13.1}Al_{14.1}$ (at.%), only marginally met the specification. Trace quantities of Ti (2.6 at.%) and Hf were detected, and considerable amounts of the interstitials were found as well; (O: 0.076 wt.% [760 ppmw]; N: 0.007 wt.% [70 ppmw]; and C: 0.025 wt.% [260 ppmw], respectively). The high oxygen and carbon content of the liner is indicative that the as-cast liners were most likely not fully amorphous. Any crystalline content or impurity inclusions would have rendered them brittle.

Dissolution of Fe would certainly lower the melting point of the metallic glass whereby its ability to flow is improved. However, it is interesting to note that the mostly metallic glass coating is completely devitrified. This is quite expected because even though the required high cooling rates may be present on the free surface to quench the coating into an amorphous state, the shift away from the intended alloy composition would likely degrade the alloy’s glass-forming ability.

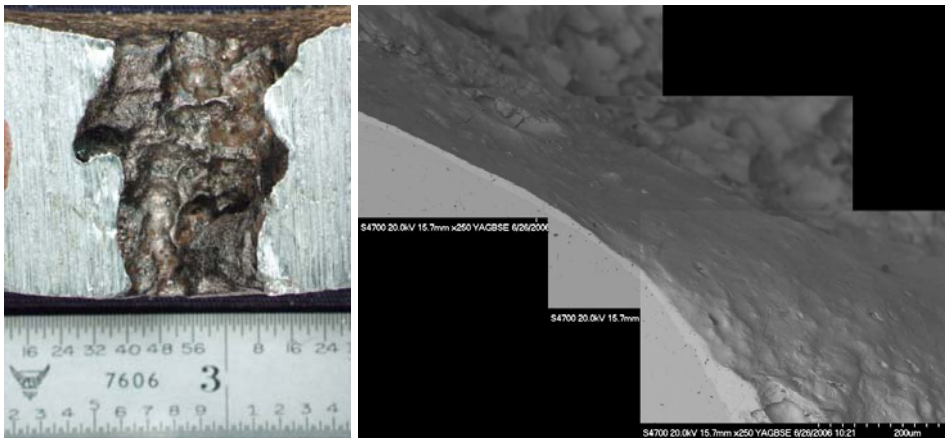

Figure 4. Enlarged views of the witness plate showing the metallic glass coating on the surface.

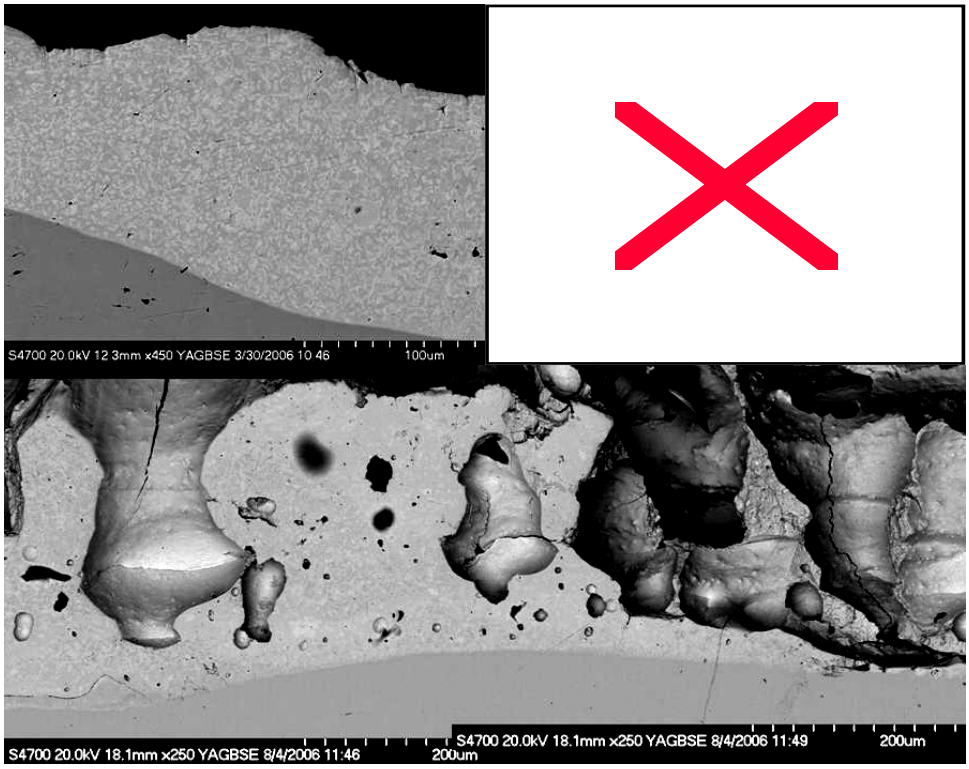

Figure 5. Examples of devitrified microstructure, interfacial cracking, and voids in the coating layer.

CONCLUSIONS

A study was conducted to evaluate the effectiveness of a Zr-based bulk metallic glass as a shaped charge liner. Results show that the liner behaved similar to particulating jets made from pressed powder liner materials. As revealed by flash X-ray radiographs and relatively poor penetration results in shots #3618 and #3619, it was surmised that the liner particulates in a highly nonuniform manner. Jet formation was asymmetric and the particles in the jet were nonuniform in size and dispersion.

It was found that the liners were non-precision quality and contained impurities that rendered them partially crystalline both of which contributed to their unremarkable performance. This may be attributed to poor quality control of liner dimensions, trapped porosity, imprecise composition, and high oxygen content.

However, these preliminary tests revealed key aspects of the fundamental penetration behavior of bulk metallic glasses in a shaped charge configuration. The interaction between the metallic glass and steel plate is undergoing further investigation. Similarly, additional tests with higher quality liners including better dimensional tolerances, alternate geometries (to subject the liner to lower strains, strain rates, pressure, and temperature) and lower impurity levels are being considered.

ACKNOWLEDGMENTS

The authors would like to thank Mr. Kenneth Willison of the U.S. ARDEC, Picatinny Arsenal, NJ, for providing us with the liners. We would also like to recognize Mr. Steven Aubert of ARL for performing the Vitreloy 106-OCTOL compatibility test and loading the explosive charges. Kudos is due to Messrs. David Weeks, Jack Koontz, and the technical staff of ERF 9. We further thank Messrs. George Dewing, Daniel Lozier, and Justin Pritchett of ARL for sectioning and cleaning of the target plates, metallographically preparing the sections, and microscopy analyses of surfaces.

REFERENCES

[1] Walters, W. P.; Zukas, J. Fundamentals of Shaped Charges, CMC Press, Baltimore, MD, 1998.
[2] W.P. Walters, P. Peregino, R. Summers, D. Leidel, A study of jets from unsintered-powder metal lined nonprecision small-caliber shaped charges; ARL-TR-2391; U.S. Army Research Laboratory: Aberdeen Proving Ground, MD, February 2001.
[3] Hao Li, unpublished results, Michigan Technological University, Houghton, MI, July 2005.
[4] Howmet Corporation, now a division of ALCOA, private communication, Whitehall, MI, no date.
[5] W. L. Johnson, Bulk glass-forming metallic alloys: Science and Technology, *MRS Bulletin*, **24**, 42-56, (1999).